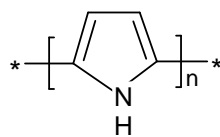


## CHAPTER 6 CONDUCTIVITY THEORY AND EXPERIMENT

### 6-1 Materials

The structure of polypyrrole is depicted in Figure 6-1. The material was synthesized electrochemically and purchased from Aldrich and BASF. Carbon fibre was procured from the Department of Mechanical Engineering at the University of Strathclyde. The general structure is shown in Figure 6-2. The thermoplastic polymer which was primarily utilised in these studies was a commercial poly(ethersulfone) based copolymer (PES) (supplied by Cytec Engineered Materials). The structure can be seen in the materials section in Chapter 4. Graphite 3775 was the nanographite material used in this study (supplied by Asbury Graphite Mills, USA). It is an intercalated natural flake graphite which has been exfoliated, compressed, and then milled to an average particle size of 5- $\mu\text{m}$ . The surface area has been increased over that of an equivalent grade of untreated natural flake graphite of the same particle distribution. Elicarb multi-wall carbon nanotubes were supplied by Thomas Swan (County Durham). Carbon black, (Vulcan XC72 and Vulcan XC605) was supplied by Cabot (Cheshire). TTF TCNQ (Tetrathiafulvelene 7,7,8,8-Tetracyanonitroquinodimethane salt) was supplied by Sigma Aldrich – the structure is displayed in Figure 6-3. The  $\beta$  form of Copper(II) phthalocyanine, with a 97 % dye content was supplied by Sigma Aldrich. The structure can be seen in Figure 6-4. PEEK poly(etheretherketone) and PEKK poly(etherketoneketone); structures shown in Figure 6-5 and Figure 6-6, were supplied by Cytec Engineered Materials.

In addition, for the epoxy resin studies, diglycidyl ether of bisphenol F (PY306) and triglycidyl ether of para-aminophenol (MY0510) were provided by Cytec Engineered Materials; the curing agent, 4,4'-diamino diphenyl sulfone (DDS) was supplied by Sigma-Aldrich. Chemical structures are shown in Figure 6-7, Figure 6-8 and Figure 6-9, respectively.



**Figure 6-1 – Polypyrrole**

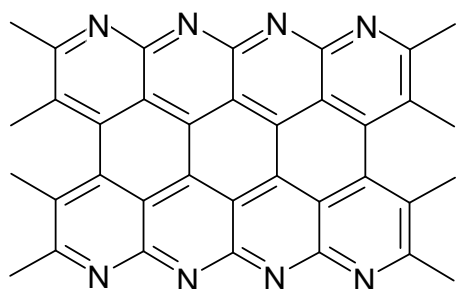
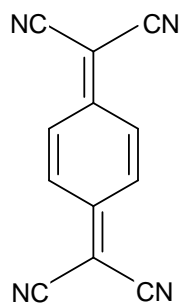
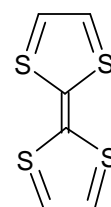


**Figure 6-2 – Carbon fibre**



**TCNQ**



**TTF**

**Figure 6-3– TTF TCNQ molecules**

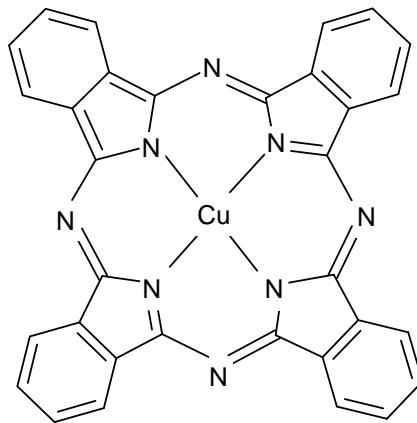


**Figure 6-4 – Cu(II) phthalocyanine**

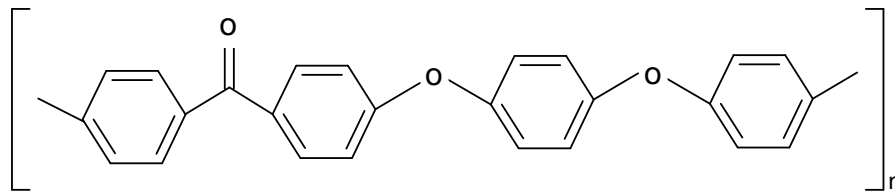


**Figure 6-5 – PEEK**

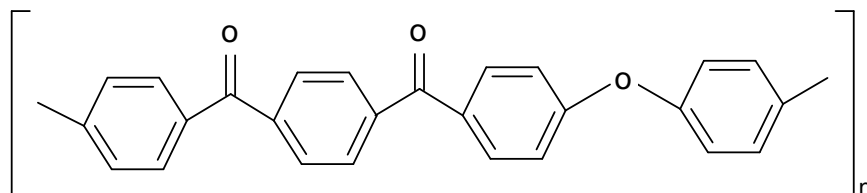


**Figure 6-6 – PEKK**

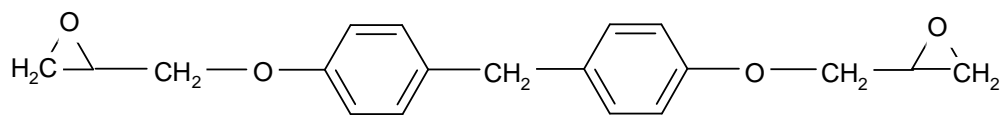


**Figure 6-7 – PY306**

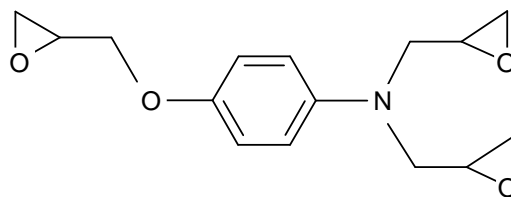


**Figure 6-8 – MY0510**

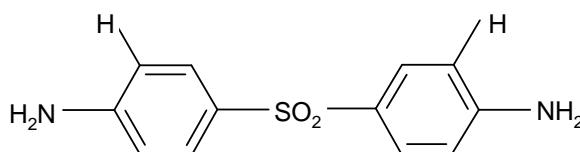


**Figure 6-9 - 4'4'-DDS**

## 6-2 Experimental Methods

In this chapter various approaches are considered for the enhancement of the electrical conductivity of thermoplastic polymer materials – specifically PES-based co-polymer, PEEK and PEKK – which might be used as fibres in composite fabrication.

The approaches which will be considered are:-

- Incorporation of intrinsically conductive polymer.
- Incorporation of carbon fibre.
- Incorporation of nanographite platelets.
- Incorporation of nanographite platelets with addition of :
  - Multi-walled carbon nanotubes
  - Carbon black
  - TTF TCNQ
  - Phthalocyanine

In addition, the effect of processing resultant materials in an extruder and a Plasti-Corder<sup>®</sup> is also considered.

In the thesis measurements are performed using a variety of different experimental methods, which are summarised in this chapter.

## **6-3 Experimental and Theory**

### **6-3-1 Polypyrrole Synthesis<sup>[1]</sup>**

Polypyrrole was synthesised electrochemically using the method adopted by Al-Arrayed *et al.*<sup>[1]</sup> The pyrrole monomer was dissolved, along with a suitable salt, in this case acetonitrile, and a current was passed through the solution.

The polymer is formed at the anode, and incorporates the salt anion at a ratio of 1:3-1:4 anions per monomer unit. The voltage was set at 0.68-0.8 Volts, relative to a saturated calomel electrode (SCE). The polypyrrole was grown in a three-electrode single-compartment cell. The anode consisted of a vapour-deposited gold layer on a chrome-on-glass substrate. Chrome was required to be used in order to ensure good adhesion of the gold to the substrate, thus avoiding many of the poor adhesion problems experienced when gold is used by itself. The voltage-current control was obtained using an EG and G Model 36 scanning potentiostat. As mentioned previously, an SCE was used as the reference electrode, with a piece of silver foil being used as the counter electrode. The electrolyte medium consisted of 0.1-0.2 mol (2.79 g–5.58 g) of silver para-toluene-sulfonate and 0.1 mol (0.68 g) of pyrrole, each dissolved in 100 mL of acetonitrile. A constant stream of nitrogen was used throughout the experiment to ensure the solutions were thoroughly degassed. Once polymerisation was complete the anode was removed from the solution, rinsed with water and air dried.

### **6-3-2 Conductivity**

#### **6-3-2-1 Percolation<sup>[2-4]</sup>**

When discussing electrical conduction it is appropriate to define the percolation threshold for electrical conductivity. Percolation is usually used to describe the spread or diffusion of something through a network. When discussing conduction, the percolation threshold is the point at which there is connectivity between the conducting elements, so

that a charge carrier can move easily through a non-conducting matrix. Below the percolation threshold, although there may be a limited range of conductivity, there is no easily defined path for the charge carriers to follow. At some point – the percolation threshold – the elements are all sufficiently close for charges to easily hop from one element to another and, as a result, the conductivity of the matrix will rapidly increase.

The percolation threshold for electrical conductivity depends very much upon the geometry of the conducting filler. Fillers with a higher aspect ratio, such as sheet-like or fibre like fillers, have an advantage in forming the conductive network in a polymer matrix over that of a filler with either a round or elliptical shape, which has a lower aspect ratio, see Figure 6-10. As an example carbon black has a percolation threshold of about 6 wt%,<sup>[2]</sup> with carbon nanotubes having a percolation threshold as low as 0.005 wt%.<sup>[3]</sup>

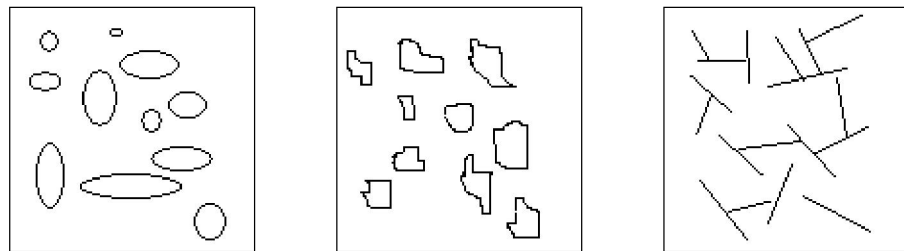


**Figure 6-10 – Schematic illustration of the effect of geometry of fillers on the formation of a conducting network**

### **6-3-2-2 Resistance and Conduction<sup>[5,6]</sup>**

The electrical resistance of a circuit component or device is defined as the ratio of the voltage applied to the electrical current, which flows through it:

$$R = \frac{V}{I} \qquad \text{Equation 6-1}$$

If the resistance is constant over a large voltage range, then Ohm's law,  $I = V/R$  can be used to predict the behaviour of the material.

Regardless of whether a material obeys Ohm's law, its resistance can be described in terms of its bulk resistivity; this is defined as the resistivity when electrical percolation occurs. In addition, there is also the surface resistivity to consider; this is the resistivity which occurs at high frequencies, and is measured on the surface of the material. Therefore, there exists the possibility for a material to be highly conductive at the surface, and insulating inside the material. The resistivity, and thus the resistance, is temperature dependent. Over sizable ranges of temperature, this temperature dependence can be predicted from a temperature coefficient of resistance.

The electrical resistance of a wire would be expected to be greater for a longer wire, less for a wire of larger cross-sectional area and would be expected to depend upon the material of which the wire is made. Experimentally, the dependence upon these properties is a straightforward one for a wide range of conditions, and the resistance of a wire can be expressed as

$$R = \frac{\rho L}{A} \quad \text{Equation 6-2}$$

where,  $\rho$  is the resistivity,  $L$  is the length and  $A$  is the cross sectional area. The factor in the equation which takes into account the nature of the material is the resistivity. The inverse of the resistivity is the conductivity. There are contexts where the use of conductivity is more appropriate. It is noted:

$$\text{Electrical conductivity} = \sigma = 1/\rho \quad \text{Equation 6-3}$$

The resistivity of materials can vary tremendously, varying in the region of 21 orders of magnitude when comparing a metal such as silver, which has a resistivity of  $1.6 \times 10^{-8}$  ohm m to a hard rubber, which has a resistivity of approx  $1-100 \times 10^{13}$  ohm m. Consequently, the way conductivity, or resistivity, is measured in practice is dependent

upon the material present. For a material thought to have a low level of conductivity it would be appropriate to take a small, thin disc of material, with dimensions as shown in Figure 6-11(a). For a material thought to have a higher degree of conductivity, it would be appropriate to take a long, thin piece of material; the dimensions of such are shown in Figure 6-11(b). In the first case, a high surface area is available with minimum thickness. The voltage is applied across the length of the material with the current being measured. In this case you minimise the resistance and maximise the current being measured. In the second case the surface area is minimised and the thickness maximised, therefore the voltage is passed through a material with small surface area with maximum thickness. In this case you maximise the resistance and in doing so the current displayed is minimised. In both cases the goal is to achieve a current which can be comfortably measured by the measurement system.

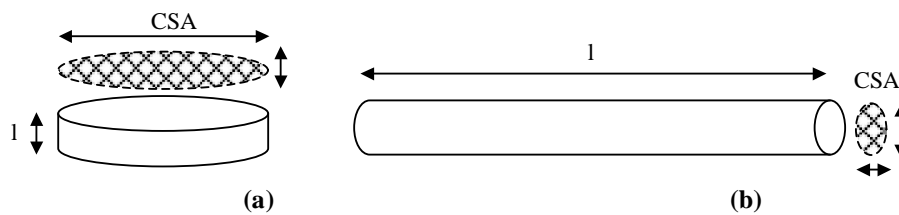


**Figure 6-11– Dimensions of materials used depending upon conductivity where  $l$  is the length and CSA is the cross-sectional area.**

### 6-3-2-3 Four-Point Probe Technique<sup>[7]</sup>

The problem of contact resistance and surface conductivity can be addressed through the use of the four-point probe technique. The experimental set-up of a four-point probe is detailed in Figure 6-12.



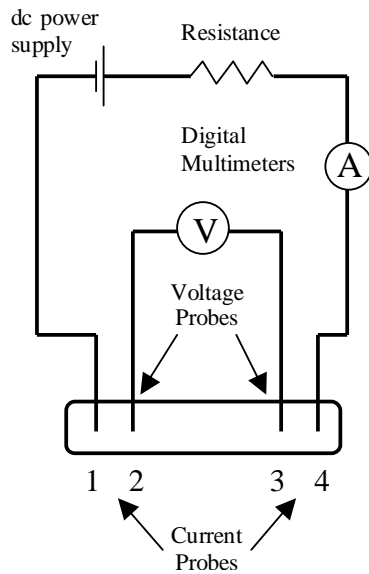


**Figure 6-12 – Four-point probe set up**

Four-point contacts are made to the sample. A current is then passed between probes 1 and 4 with the resultant voltage measured using probes 2 and 3. The test cell requires that good contact is active for all four probes and these are in practice spring loaded to achieve a constant pressure of contact with the sample to be measured. Equation 6.4 can then be used to calculate the conductivity

$$\sigma = \frac{I}{V} * \frac{1}{t * CF_1 * CF_2} \quad \text{Equation 6-4}$$

where  $\sigma$  is the conductivity,  $I$  is the current (A),  $V$  is the voltage (V) and  $t$  is the thickness (m).  $CF_1$  is the sheet resistance correction factor, which is dependent upon the sample dimensions (i.e.  $d$  is taken as the disc diameter in the case of a circular sample, and is taken as the width of the sample in the case of a rectangular sample) and the probe tip spacing ( $s$ ).  $CF_2$  is the resistivity correction factor. If the ratio of  $d/s$  is greater than 40, the sheet resistance correction factor ( $CF_1$ ) levels off at 4.5324. If the ratio is less than 40, a table is used to determine the appropriate correction factor. In the case where  $t$  is much less than  $s$  (less than 4/10 of  $s$ ), the resistivity correction factor ( $CF_2$ ) is simply equal to unity.

#### 6-3-2-4 Conductivity of Polypyrrole

In order to measure the conductivity of the various types of polypyrrole available (Strathclyde synthesised, BASF purchased and Aldrich purchased) a four-point technique was employed in all cases. The details of the technique are described in Section 6-3-2-3.

It is noted at this point that in this particular experimental set-up, when performing four-point conductivity measurements,  $t$  is much less than  $s$  in the case of the BASF and synthesised polypyrrole, therefore there is no resistivity correction factor required. In the case of the Aldrich purchased powder, an equation specifically for use when the material was pressed into 13 mm discs can therefore be created. In this project  $s$  = a constant value of 2 mm and, in the case of the discs,  $d$  = a constant value of 13 mm. From the table of correction factors, found in Appendix 1, it can be seen that there is not a  $CF_1$  value which corresponds to  $d/s=6.5$ , therefore the  $d/s$  column was plotted against the circle column and the  $CF_1$  value corresponding to  $d/s = 6.5$  was noted. The value found was equal to 3.7682. There was no  $CF_2$  value required as, in all cases, the thickness was much less than the probe tip spacing. The final equation used to determine conductivity, in the case of the Aldrich polypyrrole discs, is:

$$\sigma = \frac{I}{V} * \frac{1}{t * 3.7682} \quad \text{Equation 6-5}$$

where  $I$  is the current (A),  $V$  is the voltage (V) and  $t$  is the thickness (m). It is noted at this point that this equation is also used to determine the conductivities associated with the nanomaterial, as 13 mm pressed discs are also created for these materials.

#### 6-3-2-5 Conductivity of Carbon fibre

In the case of the carbon fibres, the conductivity of the long, thin fibres was measured using an ohmmeter; a diagram of the set-up is shown in Figure 6-13. The fibre was

attached to a glass slide using silver-loaded epoxy resin and the resistance was subsequently measured. The length of the fibre was determined using a pair of callipers, with the diameter being measured by employing a Leica optical microscope.

A Dektak IIA surface-scanning machine was also employed to determine the diameter of the carbon fibres. The needle of the machine moves along the surface until it meets the fibre. The needle then follows the contours of the fibre, and displays the thickness found on the screen. Equations 6-2 and 6-3 were then used to determine the conductivity

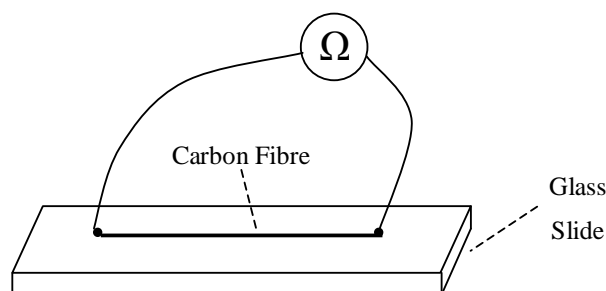


**Figure 6-13 – Set-up for conductivity measurements of carbon fibre**

### **6-3-3 Doping**

#### **6-3-3-1 Polypyrrole Doping**

Polypyrrole, see Figure 6-1, can be thought of as intrinsically conducting as an electron can move easily along the conjugated backbone of the polymer; however, the conductivity of the polymer can be substantially modified by doping. In the case of the BASF polypyrrole a 40 mm by 10 mm strip of material was used for the doping experiments. 13 mm diameter discs were used in the case of the Aldrich polypyrrole, and 10-20 mm by approximately 5 mm strips of polypyrrole were used for the Strathclyde synthesised material. The material was placed, in triplicate, in beakers containing HCl and – in the case of the BASF purchased polypyrrole – NaOH, with concentrations as shown in Table 6-1:

**Table 6-1 Concentrations of Acid/Alkali**

<b>HCl</b>	<b>HNO<sub>3</sub></b>	<b>NaOH</b>
6 M	2 M	2 M
3 M	1 M	1 M
0.6 M	0.5 M	0.2 M
		0.1 M

It is noted that before the BASF polypyrrole films were placed in the beakers of acid the mass and thickness of the samples were measured and recorded. The samples were then left for a period of 3 hours at room temperature, before rinsing with water to remove any residual acid. Conductivity measurements were then carried out using a four-point probe, as discussed in Section 6-3-2-3.

### **6-3-3-2 Carbon Fibre Doping**

Doping of carbon fibre was carried out in a similar fashion to the doping of polypyrrole, see Section 6-3-3-1, although sample preparation was slightly different. In the case of carbon fibre a single strand was removed from the bulk, using tweezers, and attached to a glass slide using silver loaded epoxy resin, as shown in Figure 6-13. Araldite<sup>®</sup> rapid, fast curing epoxy was initially used to attach 2 segments of a glass slide to a complete glass slide. The fibre could then be attached across the gap created using silver loaded epoxy resin. The slide was then placed in beakers of acid, for a 3 hour period – the concentrations of the acids involved are shown in Table 6-2. An ohmmeter could then be used to determine the conductivity of the fibres; this is detailed in Section 6-3-2-5.

**Table 6-2– Concentrations of acids involved in doping carbon fibre**

<b>HCl</b>	<b>HNO<sub>3</sub></b>
6M	7.5M
3M	3M
0.6M	0.5M

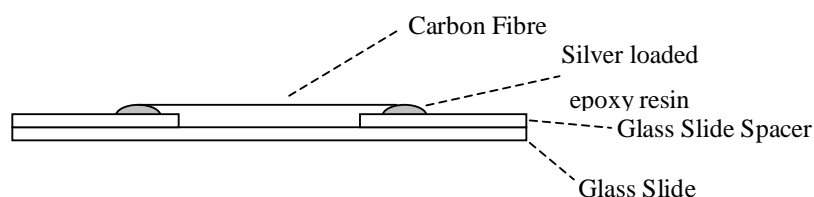


**Figure 6-14 – Carbon fibre set-up employed for doping**

#### **6-3-4 *In-situ* Polymerisation of Nanographite/ PES-based co-polymer (polymerisation was carried out by Cytec)**

In order to polymerise the PES-based co-polymer thermoplastic matrix material utilised in this project the procedure detailed in Section 4-4 was followed. In order to obtain the *in-situ* polymerised nanographite/polymer material, which was also utilised in this project, Section 6-3-5 was initially followed.

#### **6-3-5 Sonication of Nanographite**

The process involved 1 g of nanographite being weighed into a 125 mL glass jar. To this, 100 mL of sulfolane was added. Using a sonicator fitted with a microtip and set to 37 % amplitude (signal power), the tip was immersed approximately 1 cm into the nanographite/sulfolane solution. The pulse conditions used were; pulse on for 3 seconds, and pulse off for 1 second. This was carried out for 4 hours; therefore the total pulse on time is 3 hours.

The polymers used in this study were synthesized at Cytec and the details of the procedures are summarized below.

### **6-3-6 Synthesis of PEEK**

As previously discussed, the synthesis of PEEK was deemed to be proprietary, and therefore only a general description is outlined in Chapter 2, Section 2-3-2.

### **6-3-7 Synthesis of PEKK**

Again, the synthesis of PEKK was deemed to be proprietary and therefore cannot be included at this point. However it will be similar to that described for PEEK and it is therefore likely that there will be an undefined level of ionic contamination left behind in the polymer from the synthetic process.

### **6-3-8 Preparation of Epoxy Resin**

Solid PY306 was held at 60°C for 30 minutes in order to obtain the low viscosity liquid form. Release agent was spread on a mould and left in a fume hood over the duration of the experiment. 24.8 g of MY0510, 25.8 g of PY306, 30 g of PES-based co-polymer and 19.4 g of 4,4'-DDS were weighed into a beaker. It is noted at this point that an experiment with the inclusion of 10 wt% nanographite was also undertaken. In this experiment 10 g of nanographite was included at this point. The beaker was then placed in an oil bath at 120°C, with stirring, for 35-40 minutes. Upon removal from the oil bath the beaker was repeatedly moved between an oven set at 120°C and a vacuum desiccator, until no further degassing was required. The resin could then be poured out of the beaker into the mould for curing. Using a programmable oven the material was ramped to 180°C at 1 degree per minute, maintained at this temperature for a further 3 hours before ramping back to 25°C at 2 degrees per minute.

### 6-3-9 Hot-Stage Microscopy for Fibre Dissolution

The blend of epoxies and curing agent detailed in section 6-3-8 was spread on a microscope slide. A small length of fibre was then placed in the middle. The hot-stage was set to heat at 3°C per minute from room temperature to 120°C. Once the temperature was reached it was then held for a period of time to allow the fibre to dissolve. A digital camera was attached to the microscope, and allowed for videos of the dissolution to be obtained. In the dissolution experiments carried out in this report the x10 objective lens was employed.

### 6-3-10 Solution Blending and Direct Blending

#### 6-3-10-1 Solution Blending

The PES-based co-polymer / nanographite composites were prepared by a solution blending method. The PES-based co-polymer powder was first dissolved in chloroform to make a 10% solution. Different mass fractions of graphite were then added to the beaker, with dispersion aided by sonication, in order to create composites with a range of increasing nanographite loadings. The quantities of materials involved are detailed in Table 6-3. A diagram of the set up is shown in Figure 6-15.

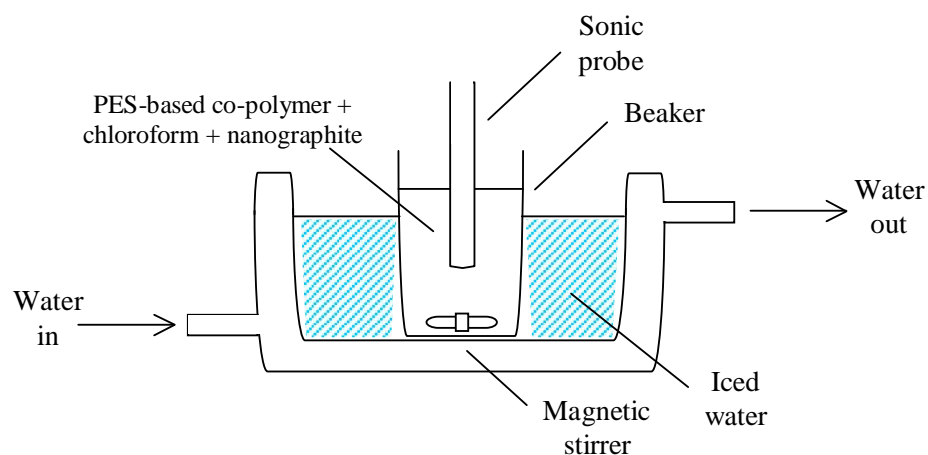


Figure 6-15– Diagram of sonication set up

Long term sonication was employed and samples were typically exposed to the sonicator for a period of 3 hours. The blends were then transferred to a circular mould with a 7 cm diameter and further solvent evaporation was carried out overnight on a desiccator attached to a vacuum pump. Samples of the composites were then ground using an electric grinder, and pressed into discs, with thicknesses ranging from 0.5 mm to 1.2 mm, using a 13 mm IR die – the load applied in order to create the discs was 5 tonnes in all cases.

**Table 6-3 – Composition of material mixtures used in solution blending**

<b>Mass of solvent / g</b>	<b>Mass of PES-based co-polymer / g</b>	<b>Mass of nanographite / g</b>	<b>% nanographite added</b>
135	15	0	0
135	14.7	0.3	2
135	14.4	0.6	4
135	14.1	0.9	6
135	13.8	1.2	8
135	13.5	1.5	10
135	12.0	3.0	20
135	10.5	4.5	30
135	9.0	6.0	40
135	7.5	7.5	50
135	6.0	9.0	60
135	4.5	10.5	70
135	3.0	12.00	80

### **6-3-10-2 Direct Blending**

#### **6-3-10-2-1 PES-Based Co-Polymer and Nanographite**

Samples of the material mixtures presented in Table 6-3 (without the addition of solvent) were blended together by mixing the appropriate ratios in 15 mL powder rounds. This method was employed in order to allow a direct comparison between directly blended samples and those samples which were sonicated. The powder mixtures were rolled for a number of hours until homogeneous mixing was achieved. 13 mm discs were then



pressed using the IR die and conductivity measurements carried out using a four-point probe.

### 6-3-10-2-2 Nanographite + Carbon Nanotubes

Increasing quantities of nanotubes were added to blends of 10 % nanographite / PES-based co-polymer; the powder mixtures were rolled for a number of hours until homogeneous mixing was achieved. The exact quantities involved are detailed in Table 6-4.

**Table 6-4 – Quantities involved in nanotube/nanographite work**

% nanotubes	% nanographite	Mass of nanotubes added / g	Mass of nanographite added / g	Mass of PES-based co-polymer added / g
0	10	0	0.5	4.5
1	10	0.05	0.5	4.45
2	10	0.10	0.5	4.40
3	10	0.15	0.5	4.35
4	10	0.20	0.5	4.30
5	10	0.25	0.5	4.25
6	10	0.30	0.5	4.20
7	10	0.35	0.5	4.15
8	10	0.40	0.5	4.10
9	10	0.45	0.5	4.05
10	10	0.50	0.5	4.00

In order to determine the maximum conductivity achievable, samples of pure nanographite and pure nanotubes were pressed into disc form and their conductivity was also determined, in triplicate.

### 6-3-10-2-3 Nanographite and Carbon Black

Conductive carbon black material, in this case XC72 and XC605, were purchased from Cabot, and increasing quantities were blended with the 10 % nanographite in PES-based co-polymer powder, the details of the quantities used are outlined in Table 6-5. All samples were based on a total sample mass of 5 g. The material was blended for a few hours on a low profile roller in order to achieve homogeneous mixing. Once blending was complete, 13 mm discs were pressed and the conductivity of each concentration of carbon black was measured, in triplicate.

**Table 6-5 – Details of quantities of materials used for nanographite/carbon black blends**

<b>% Carbon black</b>	<b>% Nanographite</b>	<b>Mass of carbon black added / g</b>	<b>Mass of nanographite added / g</b>	<b>Mass of PES-based co-polymer added / g</b>
0	10	0	0.5	4.5
10	10	0.5	0.5	4.0
20	10	1.0	0.5	3.5

### 6-3-10-2-4 Nanographite and Phthalocyanine

Copper(II) phthalocyanine, was purchased from Aldrich, and increasing quantities of the blue powder were added to the PES-based co-polymer, in order to create blends from 10 % phthalocyanine through to 100 % phthalocyanine. In addition, increasing quantities of phthalocyanine powder were blended with 10 % nanographite in PES-based co-polymer, the details of the quantities involved are displayed in Table 6-6. All samples were based on a total mass of 1 g. Again, the material was blended for a few hours on a low profile roller in order to achieve homogeneous mixing. Once blending was complete 13 mm discs were pressed and the conductivity of each concentration of phthalocyanine was measured, in triplicate.

**Table 6-6 - Details of quantities of materials used for nanographite/carbon black blends**

<b>% Phthalocyanine</b>	<b>% Nanographite</b>	<b>Mass of phthalocyanine added / g</b>	<b>Mass of nanographite added / g</b>	<b>Mass of PES-based co-polymer added / g</b>
0	10	0	0.1	0.9
20	10	0.2	0.1	0.7
40	10	0.4	0.1	0.5
80	10	0.8	0.1	0.1

**6-3-10-2-5 Nanographite and TTF TCNQ**

TTF TCNQ, seen in Figure 6-3, was purchased from Aldrich and increasing quantities of the black powder were added to the PES-based co-polymer, in order to create blends from 5 % TTF TCNQ through to 100 % TTF TCNQ. In addition, increasing quantities of TTF TCNQ powder were blended with 10 % nanographite in PES-based co-polymer; the details of the quantities involved are displayed in Table 6-7. All samples were based on a total sample mass of 1 g. Again, the material was blended for a few hours on a low profile roller in order to achieve homogeneous mixing. Once blending was complete 13 mm discs were pressed and the conductivity of each concentration of TTF TCNQ was measured, in triplicate.

**Table 6-7 - Details of quantities of materials used for nanographite/TTF TCNQ blends**

% TTF TCNQ	% Nanographite	Mass of TTF TCNQ added / g	Mass of nanographite added / g	Mass of PES-based co-polymer added / g
0	10	0	0.1	0.9
10	10	0.1	0.1	0.8
20	10	0.2	0.1	0.7
30	10	0.3	0.1	0.6
40	10	0.4	0.1	0.5
50	10	0.5	0.1	0.4
60	10	0.6	0.1	0.3
70	10	0.7	0.1	0.2

### 6-3-11 Extrusion

#### 6-3-11-1 Theory<sup>[8,9]</sup>

An extruder consists of two basic elements – The screw and the barrel which encloses the screw. The barrel is capable of being heated and cooled, and may have vents and other openings allowing specific processes to be introduced along the length of the screw, see Figure 6-16.

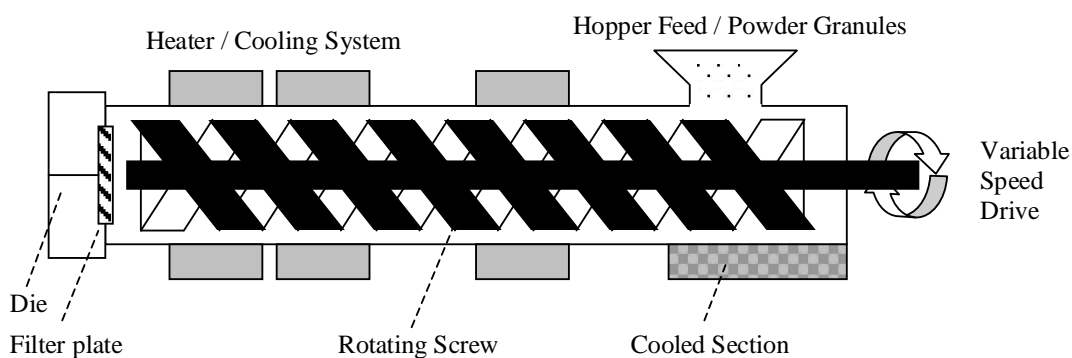


**Figure 6-16- Diagram of extruder**

The total length of the barrel can be divided, in the case of the simplest screw extruder, into three regions

- 1 The feed zone
- 2 The compression zone
- 3 The metering zone

Firstly, the feed zone is the region where the feedstock is melted by friction and compression heating. The compression zone is where the molten plastic is compressed into a viscoelastic fluid. Ideally, this region should allow the gases trapped between particles to escape, although in some cases this does not occur and a breather zone is required in addition. Finally there is the metering zone. In this region the screw is employed in order to homogenise the plastic before delivering it to the processing head.

The length of each of the previously mentioned zones will depend on the material – nylon melts very quickly so that the compression and melting can be performed in one pitch of the screw. PVC is very heat sensitive and so a compression zone, which covers the length of the barrel, is required. A typical extruder length is twenty times its diameter. The total flow can be considered in terms of three distinct effects. Firstly, the drag flow in which the polymer is pulled, by the screw, along the barrel. Secondly, the pressure flow, in which the pressure gradient moves the plug of polymer along, and finally, the leakage of the polymer past the screw, see Figure 6-17.

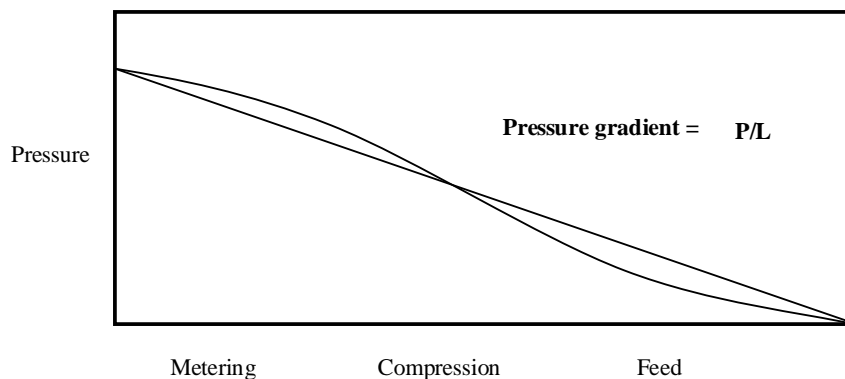


**Figure 6-17 – Pressure profile down an extruder**

There are different types of extruders available for use. The two main types are single screw extruders and twin-screw extruders. In this project a twin-screw extruder is available for use, the machine has different configurations for rotation, and these are shown in Figure 6-18.

Generally screws can be divided into 2 major categories; intermeshing and non-intermeshing. In non-intermeshing screws the separation between the screw axes is at least equal to the screw outer diameter. This can be thought of as 2 single screw extruders, which influence each other. In the intermeshing set up, the separation between the screw axes is less than the screw diameter and the screws can be in constant contact. This set up means that there is no problem with slippage of material at the wall (this is caused by the process material sticking to the screw and slipping at the barrel surface, leading to no output, as the material rotates with the screw but is not pushed forward), as the intermeshing part of one screw prevents the material in the other screw freely rotating.

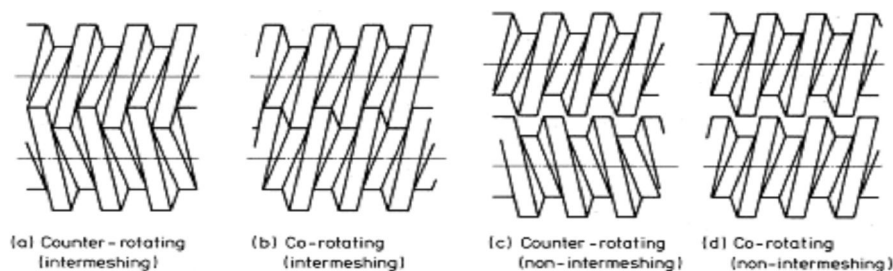


**Figure 6-18 – Twin-screw extruder configurations<sup>[10]</sup>**

In the case of a twin screw extruder, the pitch setting, which is defined as the vertical distance from any point on one thread to a corresponding point on the next successive thread, will influence the grinding ability of the system. Hence it will control the extent to which a filler will be dispersed in the polymer matrix, and also the extent to which the polymer may be degraded during the extrusion process.

Extruders have many applications and uses. They can be used for the compounding of polymer, filler, pigments and fire retardants. They can also be used for extruding

sections for windows, for extruding films, and for coating wires and textiles. In this project the extruder was utilised to create fibres containing different concentrations of nanoparticles.

### **6-3-11-2 Experimental**

Powder samples to be extruded were first of all blended together using a Stovall low profile roller. The samples were left for a few hours to ensure homogeneity of mixing. The blended material was then passed through a Prism twin Screw extruder. The temperatures of the extruder were set as follows:

270°C	270°C	260°C	260°C	250°C
<b>Die</b>	<b>Zone 4</b>	<b>Zone 3</b>	<b>Zone 2</b>	<b>Zone 1</b>

The first zone, which corresponds to the entrance to the barrel, was set at 250°C, the temperatures along the length of the barrel was set to 260°C and 270°C, with the temperature of the die being set to 270°C. The polymer powder was placed in the hopper and the drive speed adjusted to obtain a higher pressure, in order that the material came through. Once the pressure was increased and the fibre started to come through the die, the speed was decreased again. The size of the die was set at 3 mm, therefore the extruded polymer fibres were air cooled and drawn under tension onto a spool located approximately 40 cm from the die.

When increasing quantities of nanomaterial were introduced, fibres were found to break easily and it was therefore not possible to draw the material. In this case the material was taken straight from the extruder, before grinding and pressing discs.

## **6-3-12 Plasti-Corder®**

### **6-3-12-1 Theory<sup>[8,9]</sup>**

The Brabender Plasti-corder® PLE 300 utilised in this project was used as another instrument to incorporate the nanographite into the PES-based co-polymer. The instrument is connected to a computer which allows the monitoring of mixing properties such as torque and temperature, as well as control mixing parameters such as speed.

### **6-3-12-2 Experimental**

A Plasti-Corder® PLE 300 was used for sample compounding and blending. The screw speed during blending was 20 rpm. Initially, it was important to determine a useful processing temperature for the Plasti-Corder®. A sample of the PES-based co-polymer was used for this purpose. Once blended inside the barrel of the instrument, the polymer was scraped from the inside. It was found that a temperature of 290°C was sufficient in order to ensure the polymer was fully flowing. A sample of the 10 % nanographite/PES-based co-polymer blend could then be intensively blended together using the instrument. The same procedure, as detailed above, was repeated twice for the 10 % nanographite/PES-based co-polymer powder blend – initially to remove any residual PES-based co-polymer which may dilute the sample. In the case of blending the second sample it was found that the instrument cut out after a short period and therefore the blend was melted and reasonably gently mixed, it was anticipated that a more vigorous mixing would be obtained. Nonetheless, the conductivity of this material was determined.

### **6-3-13 Laboratory Scale Melt-Spinning**

The melt spinning set up consisted of a cylindrical, aluminium spinning block which had 4 small holes bored into the aluminium casing, in order to accommodate the heaters. The die was then screwed into the bottom of the cylinder and the sample added. The



temperature probe, attached to the screw top, could then be inserted into the sample. The heaters, which were capable of being heated up to 500°C, could then be placed into their holes. The heaters were then set to heat to 290°C, at which temperature the polymer was found to be dry. When the material was at the required temperature the nitrogen cylinder was switched on which forced the material through the die at the bottom of the spinning block. A fibre of the material could then be attached to a rotating, spinning cylinder shown in Figure 6-19 and Figure 6-20 which allowed the spinning of very fine fibres.



**Figure 6-19 – Pictures of melt spinning instrument**

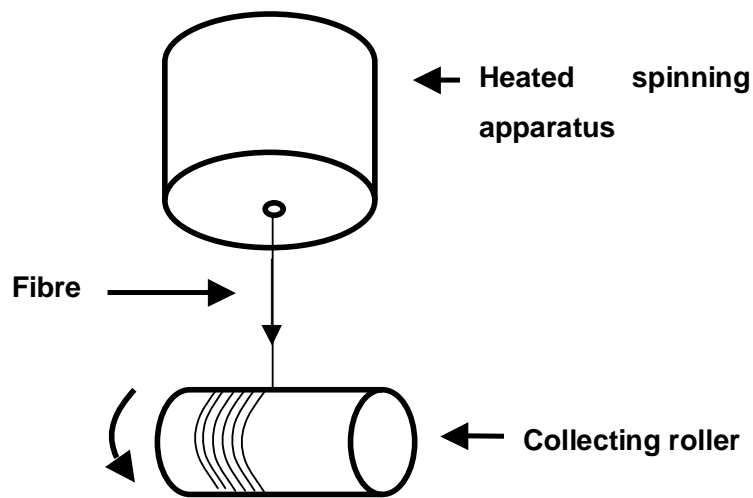


**Figure 6-20– Schematic diagram of heated spinning block**

## **6-3-14 Scanning Electron Microscopy –SEM**

### **6-3-14-1 Theory<sup>[11-13]</sup>**

Scanning Electron Microscopy, or SEM, is a very useful tool for viewing nanometre and micrometre size structures. The instrument overcomes the problems encountered with the use of traditional light microscopes, which use a series of glass lenses to bend light waves to create a magnified image, see a diagram of the set up in Figure 6-21. An SEM uses electrons to generate images. The instrument has a vacuum inside, and it is therefore necessary to prepare samples carefully to withstand the conditions. The SEM works by illuminating samples by the use of electrons. Samples therefore must be electrically conductive. To do this, a thin layer of platinum is normally deposited on the surface of the material using a sputter coater, after which an electron gun then emits a beam of high-energy electrons. The beam travels through a series of magnetic lenses, which focus the electrons to the same spot. The scan coils are designed to move the beam across the sample. As the beam hits the sample, secondary electrons are knocked off the surface, which are then collected and amplified. A picture of the surface is then created from the number of secondary electrons, which are emitted from each part of the surface.

Secondary electrons occur when the high-energy electron beam interacts with bound electrons, releasing them. Various factors contribute to the number of secondary electrons released. The atomic species present and the angle at which the electron beam interacts with the surface are both important.

It is necessary to specify that the topography of the surface greatly affects the angle to which the electron beam interacts. If a surface is uneven, there will be peaks and troughs present and this will affect the number of electrons released. If the electron beam hits a trough, electrons will collide with neighbouring surfaces, leading to a low signal and a dark spot on the image. If the beam hits a peak, the electrons have a greater chance of being detected and amplified; this leads to a bright area on the collected image.

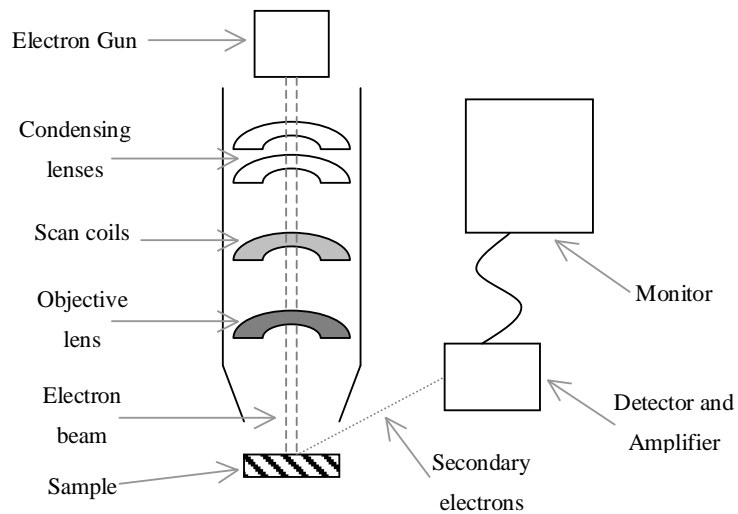


**Figure 6-21– Diagram of SEM**

### **6-3-14-2 Experimental**

Preparation of disc samples for examination involved fracturing the discs at room temperature and adhering to SEM stubs, to enable the fracture surface to be examined. A thin layer of platinum was then applied by means of an ion beam coating technique, in order to alleviate any charging problems. Examination of the specimens was carried out using a Hitachi S4500 SEM with associated PCI digital image acquisition system. Generally speaking the acceleration voltage used was 6 kV.

In the case of the nanographite powder sample, the sample was sprinkled directly onto a stub, with natural attraction forces used to hold the particles in place. Due to its nature and intimate contact with the support, it was not necessary to apply a coating to the material.

### 6-3-15 Thermal Gravimetric Analysis –TGA

#### 6-3-15-1 Theory<sup>[12-15]</sup>

Thermogravimetric Analysis (TGA) is a thermal analysis technique used to measure changes in the mass of a sample as a function of temperature and/or time. TGA is commonly used to determine polymer degradation temperatures, residual solvent levels, absorbed moisture content, and the amount of inorganic (non-combustible) filler in a polymer or composite material. Sample specimens can also be heated under different atmospheres. A typical TGA plot should look as shown in Figure 6-22.

The apparatus of a TGA instrument is relatively simple, and consists of a sensitive balance housed within a furnace equipped with a thermocouple, which measures the temperature of the sample. The sample pan is part of a sensitive electronic balance which continuously measures the mass of the sample and sends the data to the computer. The thermocouple is only a few millimetres away from the sample in the furnace so measurements are always accurate. The computer can then plot the data as a graph of percentage mass loss vs. temperature.

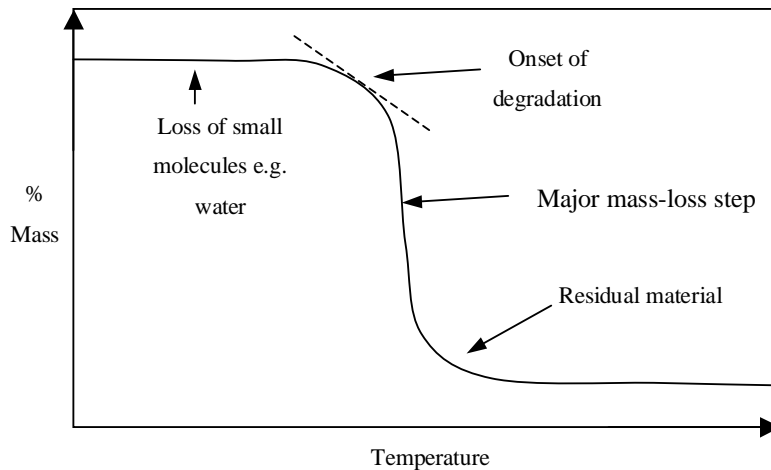


**Figure 6-22 – Typical TGA plot**

### **6-3-15-2 Experimental**

TGA measurements were made using a Shimadzu TGA-51 Thermogravimetric Analyser. Samples of approximately 20 mg in mass were examined in a platinum pan. They were subjected to an airflow rate of 50 mL min<sup>-1</sup> and a temperature ramp rate of 10°C min<sup>-1</sup> from room temperature to 800°C.

### **6-3-16 Differential Scanning Calorimetry – DSC**

#### **6-3-16-1 Theory<sup>[16-19]</sup>**

Differential scanning calorimetry (DSC) can be used to measure both the chemical and physical properties of a polymer, such as degradation and oxidation as well as the glass transition temperature, enthalpic relaxations<sup>[12]</sup> and monitoring polymer cure.<sup>[20]</sup>

There are 2 types of DSC systems in use. In power-compensated DSC, the temperature of the sample and reference pans are made identical by varying the power input to the furnaces (both sample and reference have separate furnaces). The energy, which is required for this, is a measure of the enthalpy or heat capacity changes in the sample relative to the reference.

In heat-flux DSC there is only 1 furnace involved. A metal disc encased in the furnace connects the sample and reference pans. Any enthalpic changes in the sample will be seen as a difference in temperature between the two pans.

In both types of instruments the heating rate has to be carefully chosen to minimise thermal lag and physical ageing. If the heating rate is too high a thermal lag will occur, as the specimen temperature falls behind the target; if the heating rate is too low physical ageing may occur, resulting in changes in the samples' response in later stages.

### **6-3-16-2 Experimental**

Approximately 5 mg samples were weighed into standard aluminium pans; an identical pan was used as a reference. Measurements were made using a TA Q1000 DSC. The gas used was nitrogen, and the flow rate was set to 20 mL per minute. The instrument was equilibrated at 30°C, and held for 1 minute. It was then ramped at 10°C per minute up to 500°C.

### **6-3-17 Density**

#### **6-3-17-1 Theory<sup>[21]</sup>**

The density of an object is defined as its mass per unit volume. It is an important characteristic property of a material, and can be used as an identifying tool, or to determine the purity of a material.

#### **6-3-17-2 Experimental**

Acetone was used to clean the specific gravity bottle, which was then thoroughly dried with compressed air. The empty bottle was then accurately weighed; this is mass (*a*). The bottle was completely filled with toluene and the stopper replaced. The bottle was then placed in a holder in a thermostat bath at 25°C, ensuring the water level was up to the neck of the bottle. As the mixture warmed up it started to expand and seep out of the capillary in the stopper. A tissue was used to remove the escaping liquid until no more seeped out. At this point the liquid was equilibrated and could be removed from the water bath. The bottle was dried and re-weighed; this is mass (*b*). The bottle was emptied, cleaned and dried. Approximately 1 g of sample was accurately weighed and added to the bottle; this is mass (*c*). The bottle was then filled with toluene and placed in the thermostat bath, as described above. When equilibrium was reached the bottle was removed and weighed; this is mass (*d*). The volume of the solid was calculated using

$$\text{Volume} = \frac{(b-a)-(d-c)}{\rho_{\text{toluene}}} \quad \text{Equation 6.6}$$

where  $\rho_{\text{toluene}}$  is  $0.8622 \text{ g cm}^{-3}$ . The resultant density calculation was then a simple matter of calculating mass/volume.

## 6-4 References

1. F.M. Al-Arrayed, H.L. Benham, G.G. McLeod, M.G.B.M. Jones, R.A. Pethrick, *An Investigation of Electrochemically Polymerised Pyrrole Films*. Materials Forum, 1986. **9**(4): p. 209-216.
2. S.H. Foulger, *Electrical Properties of Composites in the Vicinity of the Percolation Threshold*. Journal of Applied Polymer Science, 1999. **72**: p. 1573-1582.
3. J.K.W. Sandler, J.E. Kirk, I.A. Kinloch, M.S.P. Schaffer, A.H. Windle, *Ultra-Low Electrical Percolation Threshold in Carbon Fibre-Nanotube-Epoxy Composites*. Polymer, 2003. **44**: p. 5893-5899.
4. A. Dani, A.A. Oagle, *Percolation in Short-Fibre Composites: Cluster Statistics and Critical Exponents*. Composite Science and Technology, 1997. **57**: p. 1355-1361.
5. K. Godovskil, *Thermal and Electrical Conductivity of Polymer Materials (Advances in Polymer Science)*. 1995, Springer
6. G. Grimvall, *Thermophysical Properties of Materials*. 1995, North Holland
7. J. Chan, P. Friedberg, *EECS 143 Microfabrication Technology: Four-Point Probe Manual*, 2002
8. C. Rauwendaal, *Polymer Extrusion*. 2001, Hanser Gardner
9. C.I. Chung, *Extrusion of Polymers, Theory and Practice*. 2000, Hanser Gardner
10. N.E. Hudson, *Process Rheology Postgraduate Notes*. 2006



11. R.A. Pethrick, *Surface Analysis Final Year Lecture Notes*. 2005
12. D. Campbell, J.R. White, *Polymer Characterization. Physical Techniques*, 2000, Chapman and Hall
13. L.C. Sawyer, D.T. Grubb, *Polymer Microscopy*. 1987, Springer
14. B. Vollmert, *Polymer Chemistry*. 1973, Springer
15. H.G. Elias, *An Introduction to Polymer Science*. 1997, VCH
16. R.C. Mackenzie, *Nomenclature for Thermal Analysis – IV. Pure and Applied Chemistry*, 1985. **57**: p. 1737
17. Perkin Elmer DSC 4-instruction manual, Perkin Elmer Corporation, 1983
18. M.J. Richardson, *Comprehensive polymer science: The synthesis, characterization, reactions, & applications of polymers. Polymer properties*. 1989, Pergamon
19. N. Grassie, G. Scott, *Polymer Degradation and Stabilisation*. 1988, Cambridge University Press
20. E.A. Turi, *Thermal Characterisation of Polymeric Materials*. 1997, Academic Press
21. D.D. Ebbing, *General Chemistry*. 1996, Houghton Mifflin